

Chapter 2

Stellar Winds in Time

Brian E. Wood, Jeffrey L. Linsky, and Manuel Güdel

Abstract Exposure to stellar winds can have significant long term consequences for planetary atmospheres. Estimating the effects of these winds requires knowledge of how they evolve with time. Determining this empirically requires the ability to study the winds of stars of various ages and activity levels, but this is not easy to do as the coronal winds of solar-like stars are very hard to detect. Relevant observations are here reviewed, as well as more theoretical methods of addressing the problem.

2.1 Introduction: The Wind-Corona Connection

Besides bathing planets in electromagnetic radiation, stars also blast planets with high-speed winds. For cool main sequence stars like the Sun, the winds originate in hot ($T \sim 10^6$ K) coronae that surround the stars, heated by the release of magnetic energy generated by the dynamo in the stellar interior (Ossendrijver 2003; Charbonneau 2010). Planets in our Solar System are currently exposed to a solar wind with a mass loss rate of $\dot{M}_{\odot} = 2 \times 10^{-14} M_{\odot} \text{ year}^{-1}$ (Feldman et al. 1977). Mars is widely believed to be the planet that has been most affected by this wind. There is substantial evidence that Mars had a much thicker atmosphere in the distant past (Carr 1996; Jakosky and Phillips 2001), and erosion by the solar wind is a leading candidate for the cause of its loss (Luhmann et al. 1992; Perez de Tejada 1992; Jakosky et al. 1994; Kass and Yung 1995; Lammer et al. 2003; Terada et al. 2009; Brain et al. 2010). A recently launched NASA mission called Mars Atmosphere and Volatile Evolution spacecraft (MAVEN) will be entirely devoted to

B.E. Wood (✉)

Naval Research Laboratory, Washington, DC 20375, USA

e-mail: brian.wood@nrl.navy.mil

J.L. Linsky

JILA, University of Colorado, Boulder, CO 80309-0440, USA

e-mail: jlinsky@jila.colorado.edu

M. Güdel

Department of Astrophysics, University of Vienna, Türkenschanzstr. 17, A-1180 Vienna, Austria

e-mail: manuel.guedel@univie.ac.at

studying the effects of the solar wind on atmospheric loss when it arrives at Mars in late 2014. The effects of winds on exoplanetary atmospheres and magnetospheres is also of interest, especially for hot Jupiters that orbit very close to their stars, and which are therefore exposed to particle fluxes orders of magnitude higher than the Earth or Mars (e.g., Grießmeier et al. 2004; Khodachenko et al. 2012). This will be described in more detail in Chap. 5 (Bisikalo et al. 2014), Chap. 7 (Kislyakova et al. 2014), Chap. 8 (Vidotto et al. 2014), Chap. 10 (Alexeev et al. 2014), and Chap. 12 (Belenkaya et al. 2014) of this book.

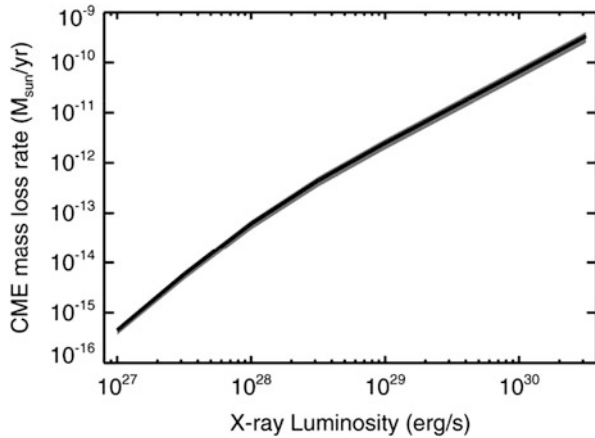
A complete understanding of how winds affect planets must start with assessments of how stellar winds evolve with time. Merely assuming that stars of all ages and spectral types have winds identical to the current solar wind is unsatisfactory. The previous chapter describes how stellar coronae change significantly with time. Therefore, it is natural to expect that the winds that emanate from these coronae could evolve significantly as well.

Young stars rotate rapidly and have very active coronae that emit copious X-ray and EUV radiation (see also Chap. 1 Linsky and Güdel 2014). This coronal emission declines dramatically as stars age and their rotation rates slow down (e.g., Güdel et al. 1997; Ribas et al. 2005). Intuitively, wind strength might be expected to evolve in concert with the coronal emission, since winds originate in stellar coronae. Thus, young stars might be expected to have more massive winds. There is undoubtedly more material heated to coronal temperatures for young, active stars, and therefore more material available to be accelerated into a wind. However, the solar example provides evidence that the wind/corona connection may not be so simple. Coronal X-ray emission from the Sun varies by a factor of 5–10 over the course of the solar activity cycle (Judge et al. 2003), but the solar mass loss rate does not vary much at all on these timescales (Cohen 2011). This demonstrates that a more active corona does not automatically lead to a stronger coronal wind.

On the other hand, active stars might also have substantial mass loss associated with sporadic coronal mass ejections (CMEs). Strong flares on the Sun are usually accompanied by dramatic, fast CMEs. These CMEs do not account for most of the solar mass loss, but flare rates and energies are known to increase dramatically with stellar activity. Young, active stars have stronger and more frequent flares, meaning that the mass loss associated with flare-associated CMEs could be much higher.

Recently Drake et al. (2013) have computed the CME mass loss rate expected for young, active stars by extrapolating a known correlation between solar flare energy and CME mass to more active stars with more frequent and energetic flares. The result is shown in Fig. 2.1, which implies that the most active stars with $\log L_X \sim 3 \times 10^{30} \text{ ergs s}^{-1}$ could have mass loss rates of $2 \times 10^4 \dot{M}_\odot$ due to CMEs alone. Limits on the percentage of a star's bolometric energy that can reasonably be expected to be spent on flares and CMEs ($\sim 10^{-3} L_{bol}$) lead Drake et al. (2013) to suggest that a more reasonable ceiling is probably closer to $2500 \dot{M}_\odot$. Nevertheless, Fig. 2.1 provides another argument for young, active stars having massive winds.

Fig. 2.1 Mass loss rate due to CMEs as a function of coronal X-ray luminosity for solar-like stars, computed by assuming that the solar-flare/CME-mass correlation can be extrapolated to younger, more active stars (After Drake et al. 2013)



2.2 Observational Constraints on Stellar Winds

2.2.1 Upper Limits from Direct Detection Techniques

Ultimately, the only way to truly establish how winds evolve with time is through observation, specifically by measuring the stellar winds of stars of various ages and activity levels. Unfortunately, this is easier said than done, because while coronal X-ray and UV emission are readily observed from stars, winds are very hard to detect. There are two direct methods of coronal wind detection that have been attempted: free-free radio emission and charge-exchange induced X-ray emission.

In the radio, observations have so far only provided upper limits for mass-loss rates (Brown et al. 1990; Lim et al. 1996; Gaidos et al. 2000). The radio arrays that they used were not sensitive enough to detect a solar-like wind around even a very nearby star, and the upper limits quoted for most non-detections are 2–3 orders of magnitude stronger than the solar wind. However, observations with new arrays such as the Atacama Large Millimeter/submillimeter Array (ALMA) or the Jansky Very Large Array (JVLA) could provide detections or at least lower upper limits. The possibility of using X-rays to search for winds has become apparent as it has been realized that most of the soft X-ray background is from our own solar wind, which emits X-rays when highly charged solar wind particles charge exchange with inflowing neutral atoms from the interstellar medium (ISM) (Lallement 2004; Koutroumpa et al. 2009). However, though potentially more sensitive than the radio technique, initial attempts to detect circumstellar wind-induced X-ray emission around nearby stars have not been successful (Wargelin and Drake 2002; Wargelin et al. 2008).

2.2.2 *Stellar Wind Measurements from Astrospheric Absorption*

The only clear detections of coronal stellar winds like that of the Sun are not of the winds themselves, but rather detections of the interactions between the winds and the ISM (Wood 2004, 2006). The interaction regions are referred to as astrospheres, analogous to the “heliosphere” that surrounds the Sun (Zank 1999). The global heliospheric structure is characterized by three boundaries: (1) the termination shock, where the solar wind is shocked to subsonic speeds, which Voyager 1 and Voyager 2 crossed at distances of 94 and 84 AU from the Sun, respectively (Stone et al. 2005, 2008), (2) the heliopause, separating the plasma flows of the solar wind and ISM, which Voyager 1 may have recently crossed at a distance of 121 AU (Gurnett et al. 2013), and (3) the bow shock, where a supersonic ISM flow would be decelerated to subsonic speeds, although recent measurements from the Interstellar Boundary Explorer (IBEX) imply that the flow may not be supersonic and therefore a bow shock may not exist (McComas et al. 2012; Zank et al. 2013; Zieger et al. 2013). Similar astrospheric structures would naturally be expected to exist around other stars with solar-like coronal winds.

The interstellar medium (ISM) immediately surrounding the Sun is only partially ionized. In the wind/ISM collision, the neutral atoms in the ISM do not interact as strongly as the ions, but they still take part through charge exchange. Modeling neutrals in the heliosphere is not easy because the charge exchange sends them entirely out of thermal and ionization equilibrium. Nevertheless, many modern heliospheric modeling codes have become sufficiently sophisticated to properly model the neutrals, starting with work by Baranov and Malama (1993, 1995) and Zank et al. (1996). These models predict that the heliosphere will be permeated by various populations of hot hydrogen atoms, defined by the region of the heliosphere in which charge exchange is occurring. Particularly important is H I created just beyond the heliopause, where the interstellar matter is decelerated, compressed, and heated relative to the undisturbed ISM. This region in the outermost heliosphere has been called the hydrogen wall.

The hydrogen wall can produce a detectable absorption signature in UV spectra of the H I Lyman- α lines of nearby stars from the Hubble Space Telescope (HST), if absorption from the ISM itself is not so broad as to obscure the heliospheric absorption. Furthermore, the observed lines of sight not only pass through our heliosphere, but they also pass through the astrospheres of the observed stars. Thus, it is also possible to detect astrospheric Lyman- α absorption, and thereby indirectly detect solar-like stellar winds. The first detection of hydrogen wall absorption was in HST observations of the two stars in the very nearby binary α Cen (G2 V + K1 V). Figure 2.2 shows the Lyman- α spectrum of α Cen B (Linsky and Wood 1996). The upper solid line is an estimate of the intrinsic Lyman- α emission line profile from the star. Intervening H I gas between HST and the star absorbs much of this Lyman- α emission, resulting in the very broad absorption line centered at about 1215.61 Å in the figure. Much narrower and weaker absorption is also seen from

neutral deuterium (D I) at 1215.27 Å. Most of the intervening H I and D I between us and the star is interstellar, but the ISM cannot account for all of the H I absorption.

When the H I absorption line is forced to have a central velocity and temperature consistent with the central velocity and width of the D I Lyman- α absorption, the ISM H I absorption ends up too narrow to fit the data. This indicates that there is excess H I absorption on both sides of the absorption that cannot be interstellar. The excess on the red side of the line is due to heliospheric absorption. The reason for the redshift is due to deceleration and deflection of ISM neutrals as they approach the heliopause, which results in a redshift from our perspective inside the heliosphere. Conversely, from our perspective outside the astrospheres, astrospheric absorption should be blueshifted.

Thus, the blue side excess absorption in Fig. 2.2 is astrospheric, as first demonstrated by Gayley et al. (1997). Note that the same excess is also observed towards both α Cen A and α Cen B, as expected since both members of the binary are close enough that they will lie within the same astrosphere, meaning that the astrospheric absorption seen towards both stars is indicative of the combined winds of both stars. Many HST Lyman- α observations of solar-like stars have been analyzed to identify those with detectable heliospheric and/or astrospheric absorption (Dring et al. 1997; Wood et al. 1996, 2000a, 2005b).

Even though all observed lines of sight will pass through the heliosphere and the astrosphere of the observed star, the absorption signatures of these structures are not always detectable. One potential cause for non-detections is a high ISM H I column density, leading to broad ISM Lyman- α absorption, which can obscure the heliospheric and astrospheric absorption. Another factor is the orientation of the line of sight with respect to the upwind direction of the ISM flow in the stellar (or solar)

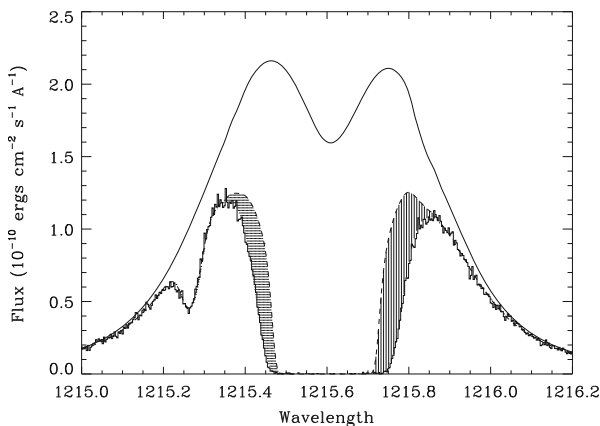


Fig. 2.2 HST Lyman- α spectrum of α Cen B, showing broad H I absorption at 1215.6 Å and D I absorption at 1215.25 Å. The *upper solid line* is the assumed stellar emission profile and the *dashed line* is the ISM absorption alone. The excess absorption is due to heliospheric H I (*vertical lines*) and astrospheric H I (*horizontal lines*) (After Linsky and Wood 1996)

rest frame. This is particularly apparent for heliospheric absorption, where many lines of sight have been observed with different angles from the upwind direction in the solar rest frame, demonstrating that the absorption is easiest to detect in upwind directions, consistent with model predictions (Wood et al. 2005b). A final major factor that applies solely to astrospheric detectability is the nature of the ISM surrounding the star. Although neutrals are present in the ISM around the Sun, this is actually not typical for stars within 100 pc. The Sun is within a region called the Local Bubble, in which most of the ISM is fully ionized (Lallement et al. 2003; Welsh et al. 2010, 2013). An astrosphere surrounded by a fully ionized ISM will contain no neutral H to produce Lyman- α absorption.

There are currently only 7 lines of sight with clear detections of heliospheric hydrogen wall absorption, all within 75° of the upwind direction of the ISM flow seen by the Sun (Wood et al. 2005b). The hydrogen wall neutrals are formed by charge exchange outside the heliopause, but it should be mentioned that in very downwind directions absorption from neutrals created by charge exchange in the inner heliosheath in between the termination shock and heliopause can become detectable. This broader but much shallower absorption signature has been clearly detected for 4 lines of sight within 20° of the downwind direction (Wood et al. 2007, 2014a) with an additional questionable detection towards Sirius (Izmodenov et al. 1999; Hébrard et al. 1999).

All 14 detections of astrospheric Lyman- α absorption are of the hydrogen wall variety, and ten are for main sequence stars like the Sun. Among these ten stars, the best analog for a young Sun is π^1 UMa, a 500 Myr old G1.5 V star (Wood et al. 2005b, 2014b). Figure 2.3 shows the Lyman- α spectrum for π^1 UMa, zooming in on the blue side of the line where the astrospheric absorption is detected. The amount of absorption will correlate with the strength of the stellar wind, but extracting a stellar mass loss rate from the Lyman- α data requires the assistance of hydrodynamic models of the astrosphere, such as the one in Fig. 2.4 for π^1 UMa, computed assuming a mass loss rate of $\dot{M} = 0.5\dot{M}_\odot$.

Astrospheric models like that in Fig. 2.4 are extrapolated from a heliospheric model that successfully reproduces heliospheric absorption, specifically a multi-fluid model described by Wood et al. (2000b). These models assume the same ISM characteristics as the heliospheric model, with the exception of the ISM flow speed in the stellar rest frame. Computing this speed requires knowledge of the star's unique space motion vector and the flow vector of the surrounding ISM. Stellar proper motions and radial velocities are very well known for the nearby stars with detected astrospheric absorption, so that is not an issue. The ISM flow vector varies somewhat from place to place, resulting in multiple ISM absorption components towards some stars, suggestive of multiple small, warm clouds in the solar neighborhood (Redfield and Linsky 2008). However, the velocity components are generally not widely separated, implying that the velocity vector of the cloud surrounding the Sun is a reasonable estimate of the ISM vector appropriate for other nearby stars. For π^1 UMa, for example, we estimate that the star sees an ISM wind speed of 34 km s^{-1} , compared to 23.8 km s^{-1} for the Sun (Redfield and Linsky

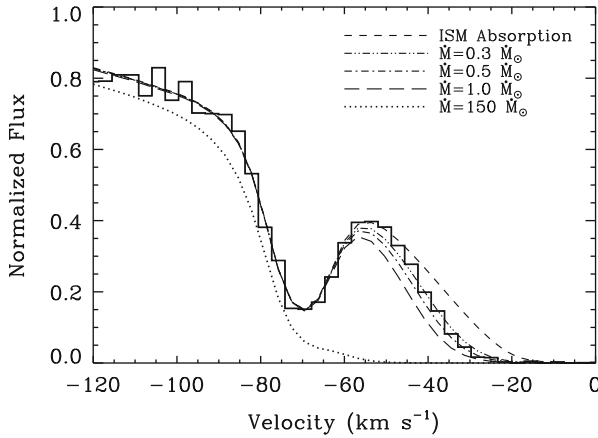


Fig. 2.3 The blue side of the Lyman- α absorption line of π^1 UMa, plotted on a heliocentric velocity scale. The absorption at -70 km s^{-1} is from D I. Since the ISM absorption cannot explain all of the H I absorption, the excess is assumed to be from the stellar astrosphere. The astrospheric absorption signature is compared with absorption predictions from four hydrodynamic models of the astrosphere, assuming four different mass-loss rates for π^1 UMa, after the astrospheric absorption is added to that of the ISM (After Wood et al. 2014b)

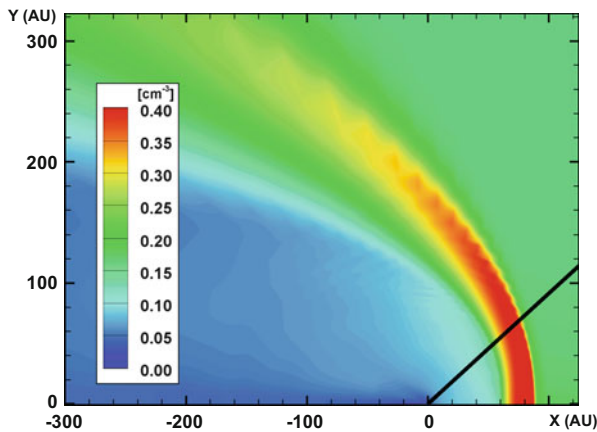


Fig. 2.4 The H I distribution of a hydrodynamic model of the π^1 UMa astrosphere, assuming $\dot{M} = 0.5\dot{M}_\odot$, which leads to the best fit to the data in Fig. 2.3. The star is at the origin, and the ISM is flowing from the right in this figure. The hydrogen wall is the parabolic shaped high-density region stretching around the star. The *black line* indicates our line of sight to the star (After Wood et al. 2014b)

2008), with our line of sight to the star lying 43° from the upwind direction, as shown in Fig. 2.4.

The astrospheric models are computed assuming different stellar wind densities, corresponding to different mass loss rates, and the Lyman- α absorption predicted by these models is compared with the data to see which best matches the observed

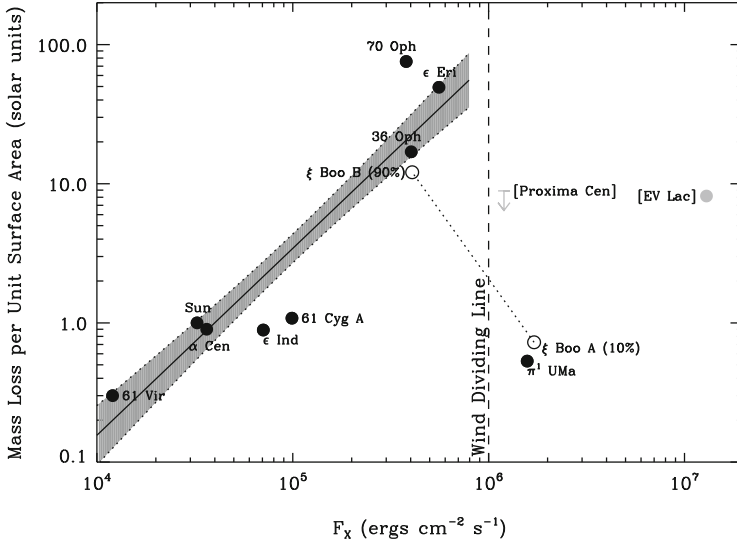


Fig. 2.5 A plot of mass loss rate (per unit surface area) versus X-ray surface flux for all main sequence stars with measured winds. Most of these are solar-like G and K stars, but the two with square-bracketed labels are M dwarfs. Separate points are plotted for the two members of the ξ Boo binary, assuming ξ Boo B accounts for 90 % of the binary’s wind, and ξ Boo A only accounts for 10 %. A power law, $\dot{M} \propto F_X^{1.34 \pm 0.18}$, is fitted to the less active stars where a wind/corona relation seems to exist, but this relation seems to fail for stars to the right of the wind dividing line in the figure (After Wood et al. 2014b)

astrospheric absorption. Figure 2.3 shows the astrospheric absorption predicted by four models of the π^1 UMa astrosphere, assuming four different stellar mass loss rates. The model with half the solar mass loss rate shown in Fig. 2.4 is deemed the best fit to the data (Wood et al. 2014b). Uncertainty in stellar wind speeds and surrounding ISM properties leads to substantial uncertainties in mass loss rates measured in this manner. Quantifying these errors is difficult, but a factor of two is a reasonable estimate for the resulting \dot{M} uncertainty. Mass loss rate estimates have been made in this way for all of the astrospheric detections (Wood et al. 2002, 2005a). Focusing on main sequence stars, Fig. 2.5 shows mass loss rates (per unit surface area) plotted versus coronal X-ray surface flux (Wood et al. 2014b). For the low-activity stars, mass loss increases with activity in a manner consistent with the $\dot{M} \propto F_X^{1.34 \pm 0.18}$ power law relation shown in the figure. For the ξ Boo binary, in which (like α Cen) the two members of the binary will share the same astrosphere, Fig. 2.5 indicates how the binary’s combined wind strength of $\dot{M} = 5\dot{M}_\odot$ is most consistent with the other measurements if 90 % of the wind is ascribed to ξ Boo B, and only 10 % to ξ Boo A.

The connection between coronal activity and stellar winds appears to be a complex one. The Sun does not show a correlation of \dot{M} with F_X , with \dot{M} varying

irregularly by less than a factor of two while the X-ray flux varies by a factor of 10 over the solar cycle (Wang 2010; Cohen 2011), possibly due to the suppression of mass flux by closed magnetic field regions where the density and X-ray emission are large. The $\dot{M} \propto F_X^{1.34 \pm 0.18}$ relation may result from the steep dependence of mass flux on X-ray luminosity in CMEs, which Drake et al. (2013) predict to be an important mass-loss mechanism in active stars but not the Sun. However, above an activity level corresponding to $\log F_X = 10^6 \text{ erg cm}^{-2} \text{ s}^{-1}$ this relation seems to fail, a boundary marked by a “Wind Dividing Line” in Fig. 2.5. Highly active stars above this limit appear to have surprisingly weak winds. This is suggested not only by the two solar-like G stars above the limit, ξ Boo A and π^1 UMa, but also for the two active M dwarfs above the limit, which have very modest mass loss rates. For Proxima Cen (M5.5 V), we only have an upper limit of $\dot{M} < 0.2 \dot{M}_\odot$ (Wood et al. 2001), while for EV Lac $\dot{M} = 1 \dot{M}_\odot$ (Wood et al. 2005a).

The apparent failure of the wind/corona correlation at the wind dividing line may indicate a fundamental change in magnetic field topology at that stellar activity level. Such a change is also suggested by observational evidence that very active stars usually have stable, long-lived polar starspots (Schrijver and Title 2001; Strassmeier 2002), in contrast to the solar example where sunspots are only observed at low latitudes. Perhaps the polar spots are indicative of a particularly strong dipolar magnetic field that envelopes the entire star and inhibits stellar wind flow, thereby explaining why very active stars have surprisingly weak winds. Very active stars may also be enveloped with strong toroidal fields as well (Donati and Landstreet 2009).

Given that young stars are more active than old stars (e.g., Ribas et al. 2005), the correlation between mass loss and activity indicated in Fig. 2.5 implies an anticorrelation of mass loss with age. The following relation between stellar X-ray flux and age for solar-like stars has been discovered by Ayres (1997): $F_X \propto t^{-1.74 \pm 0.34}$. Combining this with the power law relation from Fig. 2.4 yields the following relation between X-ray flux and age: $\dot{M} \propto t^{-2.33 \pm 0.55}$ (Wood et al. 2005a). Figure 2.6 shows what this relation suggests for the history of the solar wind, and for the history of winds from any solar-like star for that matter. The truncation of the power law relation in Fig. 2.5 near $F_X = 10^6 \text{ erg cm}^{-2} \text{ s}^{-1}$ leads to the mass-loss/age relation in Fig. 2.6 being truncated as well at about $t = 0.7 \text{ Gyr}$, slightly older than the age of the Hyades cluster. The plotted location of π^1 UMa in Fig. 2.6 indicates what the solar wind may have been like at times earlier than $t = 0.7 \text{ Gyr}$. Despite the Wind Dividing Line, the stellar wind measurements suggest that winds of younger stars are generally stronger than the solar wind (at least for $t > 0.7 \text{ Gyr}$), making it more likely that winds have significant erosive effects on planetary atmospheres over time. Analyses of lunar surface soils have also suggested a stronger solar wind in the past, though quantifying the effect is difficult from such data (e.g., Geiss 1974).

Before concluding, it should be said that inferences about the history of the solar wind from stellar astrospheric observations would certainly benefit from more data. The mass-loss/activity and mass-loss/age relations are based on only a handful of astrospheric detections. More detections would be especially desirable at high

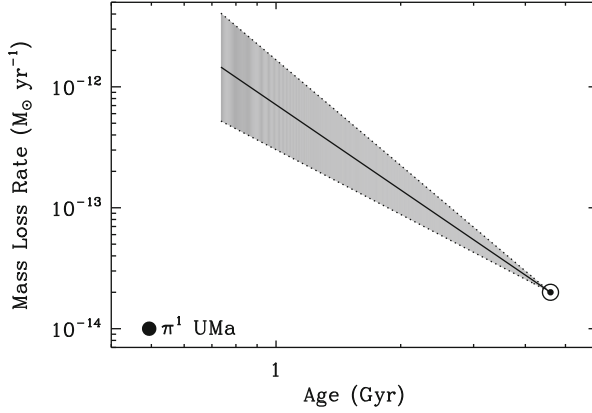


Fig. 2.6 The mass loss history of the Sun inferred from the power law relation in Fig. 2.5. The truncation of the relation in Fig. 2.4 means that the mass-loss/age relation is truncated as well. The low mass loss measurement for π^1 UMa suggests that the wind weakens at $t \approx 0.7$ Gyr as one goes back in time

activity levels to better determine what the solar wind was like when the Sun was very young and active. The Space Telescope Imaging Spectrograph (STIS) on HST is the only current instrument capable of observing the Lyman- α spectra used to detect the astrospheres.

2.2.3 *T Tauri Star Winds*

The previous subsection discussed our empirical knowledge about the winds of stars on the main sequence, which are expected to be analogous to the coronal wind of the Sun. However, very early in their history planets could also be affected by stellar winds that may be of a somewhat different character, due to the presence of a protoplanetary disk, and accretion of that disk onto the star.

Pre-Main-Sequence stars are well known to be extremely active in all stages of their evolution (Class I protostars, classical and weak-line T Tauri stars); a telltale signature is their high level of X-ray luminosity, corresponding to a saturation regime with $L_X/L_{bol} = 10^{-4} - 10^{-3}$ (e.g., Preibisch et al. 2005; Güdel et al. 2007), very high plasma temperatures (e.g., Telleschi et al. 2007), and frequent strong flares (Wolk et al. 2005). These features are taken as evidence that basically the same type of magnetic coronal structure is present and similar magnetic energy release mechanisms are at work in these objects as in main-sequence stars. By analogy, then, wind mass loss from the stellar surface may follow the trends seen in main-sequence stars. If indeed wind mass loss is suppressed in the most active stars, then we expect this to apply to Pre-Main-Sequence stars as well.

What is the observational evidence? The situation is complicated by the presence of several types of winds in disk-surrounded Pre-Main-Sequence stars; in view of the many open challenges to interpret the observations, we only briefly touch on some suggestive evidence. One manifestation of gas flows are the optically revealed bi-polar jets seen in young stellar objects; jets flow at velocities of several hundred km s^{-1} but are thought to be related to the presence of accretion in a protostellar or protoplanetary disks, evidenced by a correlation between accretion rate and mass-loss rate (Hartigan et al. 1995). Jets are probably launched magnetohydrodynamically at the star-disk interface or from the inner disk (Königl and Pudritz 2000; Shu et al. 2000). A second component, spectroscopically identified as a low-velocity wind with velocities of a few km s^{-1} , is likely related to X-ray or ultraviolet-induced photoevaporation of the disk surface at several AU to tens of AU from the central star (Alexander et al. 2004; Ercolano et al. 2008), generating a wide-angle wind that may carve out cavities in protostellar envelopes (Arce et al. 2013).

The question then is how a coronal wind escapes from the star, how it interacts with the jets and photoevaporative winds further out, and whether it energetically competes with those latter flows. The role of accretion in launching any of these wind components still also needs clarification. For example, Kwan et al. (2007), proposed that the emission profile of the He I $\lambda 10830$ line arises from some sort of stellar wind in most observed Pre-Main-Sequence stars, although the presence of these features exclusively in the presence of disks suggests an accretion-powered wind. The most likely origins of these winds are the stellar polar regions above the magnetic funnel flows (Kwan et al. 2007). Direct evidence for ionized stellar winds was also suggested in far-ultraviolet observations by Dupree et al. (2005). P Cygni-type line profiles, asymmetries and absorption indicated the presence of $\approx 300,000 \text{ K}$ winds with velocities of order 400 km s^{-1} in the classical T Tauri stars TW Hydrae and T Tauri. The mass-loss rates would then reach levels of 10^{-12} to $10^{-11} M_{\odot} \text{ year}^{-1}$. However, a re-analysis of these data by Johns-Krull and Herczeg (2007) puts this interpretation in doubt; it sets an upper limit of only $10,000\text{--}30,000 \text{ K}$ to the wind temperature and implies that the ionization state is due to photoionization, making these outflows different from solar-type coronal winds.

Magnetized stellar winds have also been suggested for such disk-surrounded Pre-Main-Sequence stars to explain their relatively slow rotation, as an alternative to the problematic magnetic disk-locking mechanism. For example, Matt and Pudritz (2005) postulated accretion-powered massive winds escaping into large solid angles with open fields anchored in the stellar polar regions, with $\dot{M}_w \approx 0.1 \dot{M}_a$, where \dot{M}_a is the stellar accretion rate. Wind mass-loss rates of order $10^{-10} M_{\odot} \text{ year}^{-1}$ or even more should therefore be expected. More sophisticated models of this kind were elaborated in a series of studies by Matt et al. (2012). The accretion-related launching mechanisms of stellar winds have also been considered by Cranmer (2008) suggesting turbulence-driven polar winds energized by accretion. We refer to the contribution in Chap. 3 by Lüftinger et al. (2014) in this volume for further details.

2.3 Expectations from Theoretical Models

Given the difficulty of studying coronal winds observationally, it is worthwhile to assess what can be inferred about wind evolution from theory. For cool main sequence stars, proposed wind acceleration mechanism include thermal pressure-driven winds originally proposed by Parker (1958), magnetic wave-driven winds originally proposed by Webber and Davis (1967), and magnetocentrifugally-driven winds (e.g., Vidotto et al. 2011). Most recent models include magnetic effects for the wind acceleration mechanism. We summarize here three theoretical studies that explore the different wind acceleration mechanisms and predict mass-loss rates that can be compared with observations.

Holzwarth and Jardine (2007) extended the Webber and Davis (1967) model by using thermal wind parameters (temperature, density, and magnetic field strength) that depend functionally on the stellar rotation rate. They found that for slowly-rotating stars the main driving force is thermal pressure gradients in the corona, but for fast rotators the winds are accelerated mainly by magneto-centrifugal forces. Their model is consistent with the mass-loss rates measured by Wood et al. (2005a) for slowly-rotating stars like the Sun and the most rapidly-rotating active stars (e.g., ξ Boo A and EV Lac). However, their model fails to explain the moderately-rotating K dwarfs (ϵ Eri, 36 Oph, and 70 Oph), which have mass flux rates nearly 100 times solar but coronal densities inferred from X-ray luminosities that are not sufficiently large to explain the very high mass loss rates. Since they could find no consistent set of parameters to explain both the observed very high mass-loss rates for the moderately-rotating stars and the modest mass-loss rates of the rapidly-rotating stars, they concluded that the moderately-rotating K dwarfs are uncharacteristic for the winds of cool main-sequence stars. They conclude with a model in which the mass-loss rate of a $1M_{\odot}$ star decreases by one order of magnitude between 10^6 years and the present age of the Sun.

Cranmer and Saar (2011) developed a magnetic turbulence-driven wind model in which they follow the MHD turbulence energy flux from the subphotosphere convective zone through the corona where the energy emerges as wind expansion through open magnetic field lines. Their model is physically self-consistent. For cool dwarf stars, the driving mechanism for mass outflow is primarily thermal pressure gradients, although they do include Alfvén wave pressure that dominates for giant stars. For cool dwarf stars, photospheric magnetic field strengths are close to the equipartition value with the filling factors increasing rapidly with faster rotation (Cuntz et al. 1998). For solar mass stars, their standard model predicts mass flux rates about 100 times the present Sun at ages 10^7 to 10^8 years, but with an age dependence proportional to $t^{-1.1}$ compared with the empirical relation $\dot{M} \sim t^{-2.33 \pm 0.55}$ found by Wood et al. (2005a). It is suggested by Cranmer and Saar (2011) that a steeper age dependence of \dot{M} would result from an alternative dependence of rotation rate on age. Their approach has the advantage that it is based on physical principals and empirical stellar parameters, but except for active M dwarfs like EV Lac, it provides mass flux estimates within an order of magnitude

of empirical values. They suggest that a different driving mechanism, perhaps flares and coronal mass ejections, may explain the observed large mass loss rates.

For very rapidly-rotating stars, centrifugal forces likely play an important role in driving mass loss. A recent study by Vidotto et al. (2011) considered the M4 dwarf star V374 Peg with a rotational period of 0.44 days. They solved the magnetohydrodynamic (MHD) equations in the strong poloidal magnetic field obtained from Zeeman Doppler imaging. The rapid rotation and strong magnetic fields produce a wind with a high speed, 1,500–2,300 km/s, and extremely high mass-loss rates, $3\text{--}50 \times 10^{-11} M_{\odot}$ year. These mass-loss rates are 3–4 orders of magnitude larger than solar and 2–3 orders of magnitude larger than found for the M dwarf star EV Lac by the astrospheres technique. These mass-loss rates predict short time scales for rotational braking and thus may be inconsistent with the short rotational period of the star. Despite these problems, this study shows that centrifugal forces likely play an important role in driving winds of rapidly-rotating stars.

Although these theoretical models are roughly consistent with the observations, there remain serious problems in explaining the low mass-loss rates of the active stars. We look forward to the next generation of stellar wind models that will, hopefully, better explain the present and future observations.

Conclusion

There is much room for improvement with regards to our knowledge of how stellar winds vary with time. Astrospheric Lyman- α absorption currently provides the only method to detect and measure the coronal winds of cool main sequence stars, but there are still only a handful of detections. These data are generally consistent with younger, more active stars having stronger winds, up to $\dot{M} \sim 100\dot{M}_{\odot}$ for stars about 0.7 Gyr old, increasing the likelihood that winds have significant impacts on the evolution of planetary atmospheres. However, the recent π^1 UMa measurement suggests a different regime for the wind-corona connection at earlier ages, when stars may have surprisingly weak winds. More data are clearly required to explore these issues.

Unfortunately, the astrospheric diagnostic has substantial drawbacks that make the acquisition of additional relevant measurements uncertain. In the near future UV space observatories such as the World Space Observatory-UV (WSO-UV) (see Chap. 14 by (Shustov et al. 2014)) can be used for observations. At present HST is the only observational platform capable of these observations. Obtaining HST time for these purposes is not easy, particularly since the astrospheric detection likelihood for most stars is quite low (Wood et al. 2005b). What is worse is that the reason for most non-detections (being surrounded by an ISM without neutral H) means that

(continued)

non-detections do not even provide meaningful upper limits to \dot{M} in most instances. Hopefully a more direct wind detection technique can ultimately be found without these drawbacks. Free-free radio emission from the ionized coronal winds would seem to be the most likely observational approach, though even the expanded VLA and the new ALMA array are likely to fall short of the sensitivity necessary to detect the modest winds successfully detected through astrospheric absorption. A far more sensitive radio telescope will ultimately be required to survey the stellar winds of nearby stars in the way that X-ray surveys have successfully studied the stellar coronae responsible for these winds.

Acknowledgements The authors acknowledge the support by the International Space Science Institute (ISSI) in Bern, Switzerland and the ISSI team *Characterizing stellar- and exoplanetary environments*. Support for this work was also provided by NASA through an award from the Space Telescope Science Institute (program GO-12596), which is operated by the Association of Universities for Research in Astronomy, Inc., under NASA contract NAS 5-26555. M. Güdel acknowledges support from the Austrian Research Foundation FWF NFN project S11601-N16 ‘Pathways to Habitability: From Disks to Active Stars, Planets and Life’, as well as the related FWF NFN subprojects, S116 604-N16 ‘Radiation & Wind Evolution from T-Tauri Phase to ZAMS and Beyond’.

References

- Alexander, R. D., Clarke, C. J., & Pringle, J. E. (2004). *Monthly Notices of the Royal Astronomical Society*, 354, 71.
- Alexeev, I. I., Grygoryan, M. S., Belenkaya, E. S., Kalegaev, V. V., & Khodachenko, M. L. (2014). H. Lammer & M. L. Khodachenko (Eds.), *Characterizing stellar and exoplanetary environments* (pp. 189). Heidelberg/New York: Springer.
- Arce, H. G., Mardones, D., Corder, S. A., Garay, G., Noriega-Crespo, A., Raga, A. C. (2013). *Astrophysical Journal*, 774, 39.
- Ayres, T. R. (1997). *Journal of Geophysical Research*, 102, 1641.
- Baranov, V. B., & Malama, Y. G. (1993). *Journal of Geophysical Research*, 98, 15157.
- Baranov, V. B., & Malama, Y. G. (1995). *Journal of Geophysical Research*, 100, 14755.
- Belenkaya, E. S., Khodachenko, M. L., & Alexeev, I. I. (2014). H. Lammer & M. L. Khodachenko (Eds.), *Characterizing stellar and exoplanetary environments* (pp. 239). Heidelberg/New York: Springer.
- Bisikalo, D. V., Kaygorodov, P. V., Ionov, D. E., & Shematovich, V. I. (2014). H. Lammer, & M. L. Khodachenko (Eds.), *Characterizing stellar and exoplanetary environments* (pp. 81). Heidelberg/New York: Springer.
- Brain, D., et al. (2010). *Icarus*, 206, 139.
- Brown, A., Vealé, A., Judge, P., Bookbinder, J. A., & Hubeny, I. (1990). *Astrophysical Journal*, 361, 220.
- Carr, M. H. (1996). *Water on mars*. New York: Oxford University Press
- Charbonneau, P. (2010). *Living Reviews in Solar Physics*, 7, 3. <http://www.livingreviews.org/lrsp-2010-3>
- Cohen, O. (2011). *Monthly Notices of the Royal Astronomical Society*, 417, 2592.

- Cranmer, S. R. (2008). *Astrophysical Journal*, 689, 316.
- Cranmer, S. R. & Saar, S. H. (2011). *Astrophysical Journal*, 741, 54.
- Cuntz, M., Ulmschneider, P., & Musielak, Z. E. (1998). *Astrophysical Journal*, 493, L117.
- Donati, J.-F., & Landstreet, J. D. (2009). *Annual Review of Astronomy and Astrophysics*, 47, 333.
- Drake, J. J., Cohen, O., Yashiro, S., Gopalswamy, N. (2013). *Astrophysical Journal*, 764, 170.
- Dring, A. R., et al. (1997). *Astrophysical Journal*, 488, 760.
- Dupree, A. K., Brickhouse, N. S., Smith, G. H., & Strader, J. (2005). *Astrophysical Journal*, 625, L131.
- Ercolano, B., Drake, J. J., Raymond, J. C., & Clarke, C. C. (2008). *Astrophysical Journal*, 688, 398.
- Feldman, W. C., Asbridge, J. R., Bame, S. J., Gosling, J. T. (1977). O. R. White (Ed.) *The solar output and its variation* (p. 351). Boulder: Colorado Associated University Press.
- Gaidos, E. J., Güdel, M., & Blake, G. A. (2000). *Geophysical Research Letters*, 27, 501.
- Gayley, K. G., Zank, G. P., Pauls, H. L., Frisch, P. C., & Welty, D. E. (1997). *Astrophysical Journal*, 487, 259.
- Geiss, J. (1974), D. R. Criswell & J. W. Freeman (Eds.), *Conference on lunar interactions: Interactions of the interplanetary plasma with the modern and ancient moon* (p. 110). Houston: Lunar Science Institute.
- Grieffmeier, J.-M., et al. (2004). *Astronomy and Astrophysics*, 425, 753.
- Güdel, M., et al. (2007). *Astronomy and Astrophysics*, 468, 353.
- Güdel, M., Guinan, E. F., Skinner, S. L. (1997). *Astrophysical Journal*, 483, 947.
- Gurnett, D. A., Kurth, W. S., Burlaga, L. F., Ness, N. F. (2013). *Science*, 341, 1489.
- Hartigan, P., Edwards, S., Ghandour, L. (1995). *Astrophysical Journal*, 452, 736.
- Hébrard, G., Mallouris, C., Ferlet, R., Koester, D., Lemoine, M., Vidal-Madjar, A., & York, D. (1999) *Astronomy and Astrophysics*, 350, 643.
- Holzwarth, V. & Jardine, M. (2007) *Astronomy and Astrophysics*, 463, 11.
- Izmodenov, V. V., Lallement, R., Malama, Y. G. (1999). *Astronomy and Astrophysics*, 342, L13.
- Jakosky, B. M., Pepin, R. O., Johnson, R. E., & Fox, J. L. (1994). *Icarus*, 111, 271.
- Jakosky, B. M., & Phillips, R. J. (2001). *Nature*, 412, 237.
- Johns-Krull, C. M., & Herczeg, G. J. (2007). *Astrophysical Journal*, 655, 345.
- Judge, P. G., Solomon, S. C., & Ayres, T. R. (2003). *Astrophysical Journal*, 593, 534.
- Kass, D. M., & Yung, Y. L. (1995) *Science*, 268, 697.
- Khodachenko, M. L., et al. (2012). *Astrophysical Journal*, 744, 70.
- Kislyakova, K. G., Holmström, M., Lammer, H., & Erkaev, N. V. (2014). H. Lammer, & M. L. Khodachenko (Eds.), *Characterizing stellar and exoplanetary environments* (pp. 137). Heidelberg/New York: Springer.
- Königl, A., & Pudritz, R. E. (2000). V. Mannings, A. P. Boss, & S. S. Russell (Eds.), *Protostars planets IV* (pp. 759). Tucson: University of Arizona Press.
- Koutroumpa, D., Lallement, R., Raymond, J. C., & Kharchenko, V. (2009). *Astrophysical Journal*, 696, 1517.
- Kwan, J., Edwards, S., & Fischer, W. (2007). *Astrophysical Journal*, 657, 897.
- Lallement, R. (2004). *Astronomy and Astrophysics*, 418, 143.
- Lallement, R., Welsh, B. Y., Vergely, J. L., Crifo, F., & Sfeir, D. (2003). *Astronomy and Astrophysics*, 411, 447.
- Lammer, H., et al. (2003). *Icarus*, 165, 9.
- Lim, J., White, S. M., & Slee, O. B. (1996). *Astrophysical Journal*, 460, 976.
- Linsky, J. L., & Wood, B. E. (1996). *Astrophysical Journal*, 463, 254.
- Linsky, J. L., Güdel, M., (2014). H. Lammer & M. L. Khodachenko (Eds.), *Characterizing stellar and exoplanetary environments* (pp. 3). Heidelberg/New York: Springer.
- Luhmann, J. G., Johnson, R. E., & Zhang, M. H. G. (1992). *Geophysical Research Letters*, 19, 2151.
- Lüftinger, T., Vidotto, A. A., & Johnstone, C. P. (2014). H. Lammer & M. L. Khodachenko (Eds.), *Characterizing stellar and exoplanetary environments* (pp. 37). Heidelberg/New York: Springer.

- Matt, S., Pinzón, G., Greene, T. P., & Pudritz, R. E. (2012). *Astrophysical Journal*, 745, 101.
- Matt, S., & Pudritz, R. E. (2005). *Astrophysical Journal*, 632, L135.
- McComas, D. J., et al. (2012). *Science*, 336, 1291.
- Ossendrijver, M. (2003). *A&ARv*, 11, 287.
- Parker, E. N. (1958). *Astrophysical Journal*, 128, 664.
- Perez de Tejada, H. (1992). *Journal of Geophysical Research*, 97, 3159.
- Preibisch, T., et al. (2005). *Astrophysical Journal*, 160, 401.
- Redfield, S., & Linsky, J. L. (2008). *Astrophysical Journal Supplement Series*, 673, 283.
- Ribas, I., Guinan, E. F., Güdel, M., & Audard, M. (2005). *Astrophysical Journal*, 622, 680.
- Schrijver, C. J., & Title, A. M. (2001). *Astrophysical Journal*, 551, 1099.
- Shu, F. H., Najita, J. R., Shang, H., & Li, S.-Y. (2000). V. Mannings, A. P. Boss, & S. S. Russell (Eds.), *Protostars planets IV* (p. 789). Tucson: University of Arizona Press.
- Stone, E. C., Cummings, A. C., McDonald, F. B., Heikkilä, B. C., Lal, N., & Webber, W. R. (2005). *Science*, 309, 2017.
- Stone, E. C., Cummings, A. C., McDonald, F. B., Heikkilä, B. C., Lal, N., & Webber, W. R. (2008). *Nature*, 454, 71.
- Strassmeier, K. G. (2002). *Astronomische Nachrichten*, 323, 309.
- Shustov, B. M., Sachkov, M. E., Bisikalo, D., & Gómez de Castro, A.-I. (2014). H. Lammer & M. L. Khodachenko (Eds.), *Characterizing stellar and exoplanetary environments* (pp. 275). Heidelberg/New York: Springer.
- Telleschi, A., Güdel, M., Briggs, K. R., Audard, M., & Palla F. (2007). *Astronomy and Astrophysics*, 468, 425.
- Terada, N., Kulikov, Y. N., Lammer, H., Lichtenegger, H. I. M., Tanaka, T., Shinagawa, H., & Zhang, T. (2009). *Astrobiology*, 9, 55.
- Vidotto, A. A., Jardine, M., Opher, M., Donati, J. F., & Gombosi, T. I. (2011). *Monthly Notices of the Royal Astronomical Society*, 412, 351.
- Vidotto, A. A., Bisikalo, D. V., Fossati, L., & Llama, J. (2014). H. Lammer & M. L. Khodachenko (Eds.), *Characterizing stellar and exoplanetary environments* (pp. 153). Heidelberg/New York: Springer.
- Wang, Y.-M. (2010). *Astrophysical Journal*, 715, L121.
- Wargelin, B. J., & Drake, J. J. (2002). *Astrophysical Journal*, 578, 503.
- Wargelin, B. J., Kashyap, V. L., Drake, J. J., García-Alvarez, D., & Ratzlaff, P. W. (2008). *Astrophysical Journal*, 676, 610.
- Webber, E. J. & Davis, L. J. (1967). *Astrophysical Journal*, 148, 217.
- Welsh, B. Y., Lallement, R., Vergely, J. L., & Raimond, S. (2010). *Astronomy and Astrophysics*, 510, A54.
- Welsh, B. Y., Wheatley, J., Dickinson, N., & Barstow, M. A. (2013). *PASP*, 125, 644.
- Wolk, S. J., Harnden, F. R., Jr., Flaccomio, E., Micela, G., Favata, F., Shang, H., & Feigelson, E. D. (2005). *Astrophysical Journal Supplement Series*, 160, 423.
- Wood, B. E. (2004). *Living Reviews in Solar Physics*, 1, 2. <http://www.livingreviews.org/lrsp-2004-2>
- Wood, B. E. (2006). *Space Science Reviews*, 126, 3.
- Wood, B. E., Alexander, W. R., & Linsky, J. L. (1996). *Astrophysical Journal*, 470, 1157.
- Wood, B. E., Izmodenov, V. V., Alexashov, D. B., Redfield, S., & Edelman, E. (2014a). *Astrophysical Journal*, 780, 108.
- Wood, B. E., Izmodenov, V. V., Linsky, J. L., & Malama, Y. G. (2007). *Astrophysical Journal*, 657, 609.
- Wood, B. E., Linsky, J. L., Müller, H.-R., & Zank, G. P. (2001). *Astrophysical Journal*, 547, L49.
- Wood, B. E., Linsky, J. L., & Zank, G. P. (2000a). *Astrophysical Journal*, 537, 304.
- Wood, B. E., Müller, H.-R., Redfield, S., & Edelman, E. (2014b). *Astrophysical Journal*, 781, L33.
- Wood, B. E., Müller, H.-R., & Zank, G. P. (2000b). *Astrophysical Journal*, 542, 493.
- Wood, B. E., Müller, H.-R., Zank, G. P., & Linsky, J. L. (2002). *Astrophysical Journal*, 574, 412.
- Wood, B. E., Müller, H.-R., Zank, G. P., Linsky, J. L., & Redfield, S. (2005a). *Astrophysical Journal*, 628, L143.

- Wood, B. E., Redfield, S., Linsky, J. L., Müller, H.-R., & Zank, G. P. (2005b). *Astrophysical Journal Supplement Series*, 159, 118.
- Zank, G. P. (1999). *Space Science Reviews*, 89, 413.
- Zank, G. P., Heerikhuisen, J., Wood, B. E., Pogorelov, N. V., Zirnstein, E., McComas, D. J. (2013). *Astrophysical Journal*, 763, 20.
- Zank, G. P., Pauls, H. L., Williams, L. L., & Hall, D. T. (1996). *Journal of Geophysical Research*, 101, 21639.
- Zieger, B., Opher, M., Schwadron, N. A., McComas, D. J., & Tóth, G. (2013). *Geophysical Research Letters*, 40, 2923.

Characterizing Stellar and Exoplanetary Environments

Lammer, H.; Khodachenko, M. (Eds.)

2015, XXI, 310 p. 85 illus., 50 illus. in color., Hardcover

ISBN: 978-3-319-09748-0